

## SOME SUCCESSFUL APPROACHES TO QUANTITATIVE MINERAL ANALYSIS AS REVEALED BY THE 3<sup>RD</sup> REYNOLDS CUP CONTEST

OLADIPO OMOTOSO<sup>1,\*</sup>, DOUGLAS K. MCCARTY<sup>2</sup>, STEPHEN HILLIER<sup>3</sup> AND REINHARD KLEEBOG<sup>4</sup>

<sup>1</sup> CANMET Energy Technology Centre, Natural Resources Canada, Devon, AB, Canada T9G 1A8

<sup>2</sup> Chevron ETC, Houston, TX 77042-5397, USA

<sup>3</sup> Macaulay Institute, Craigiebuckler, Aberdeen AB15 8QH, UK

<sup>4</sup> TU Bergakademie Freiberg, Institute of Mineralogy, Freiberg D-09596, Germany

**Abstract**—Details of the quantitative techniques successfully applied to artificial rock mixtures distributed for the third Clay Minerals Society Reynolds Cup (RC) contest are presented. Participants each received three samples, two containing 17 minerals each and a third containing ten minerals. The true composition of the samples was unknown to all participants during the contest period. The results submitted were ranked by summing the deviations from the actual compositions (bias). The top three finishers used mainly X-ray diffraction (XRD) for identification and quantification. The winner obtained an average bias of 11.3% per sample by using an internal standard and modified single-line reference intensity ratio (RIR) method based on pure mineral standards. Full-pattern fitting by genetic algorithm was used to measure the integrated intensity of the diagnostic single-line reflections chosen for quantification. Elemental-composition optimization was used separately to constrain phase concentrations that were uncertain because the reference mineral standards were lacking or not ideal. Cation exchange capacity, oriented-sample XRD analysis, and thermogravimetric analysis were also used as supplementary techniques. The second-place finisher obtained an average bias of 13.9%, also by using an RIR method, but without an added internal standard and with intensity measured by whole-pattern fitting. The third-place finisher, who obtained an average bias of 15.3%, used the Rietveld method for quantification and identification of minor phases (using difference plots). This participant also used scanning electron microscopy (with X-ray microanalysis) to identify minor components and verify the composition of structures used in Rietveld analysis. As in the previous contests, successful quantification appears to be more dependent on analyst experience than on the analytical technique or software used.

**Key Words**—Clay Minerals, Pure Reference Minerals, Quantitative Analysis, Reference Intensity Ratio, Reynolds Cup, Rietveld, The Clay Minerals Society, Whole-pattern Fitting.

### INTRODUCTION

Quantitative analysis of clay-bearing minerals is beset with uncertainties not generally encountered in the analysis of non-clay minerals or synthetic materials with well defined structures. In addition to the quantification problems, the presence of compositional and stacking disorders and mixed-layering in some of the most frequently observed clay minerals make positive identification difficult. The Reynolds Cup contest, named after Bob Reynolds for his great contributions to clay science, was established by Douglas McCarty, Jan Środoń and Dennis Eberl (McCarty, 2002). The idea was to create clay-bearing samples from 'pure' mineral standards typical of sedimentary rock compositions and allow interested individuals to use analytical techniques of their choice to identify and quantify the mineral phases. The choice to mimic sedimentary rock compositions was made because this is probably the most common rock type where there is a clear need, driven by both research and wide commercial interests, for

quantitative mineralogical analysis that includes clay minerals. However, because of the difficulty in obtaining suitable pure mineral standards, some deviation from this goal had to be made for practical reasons. Therefore, in the recent contest, the minerals in the samples may be found in sedimentary rocks, but not necessarily in the exact assemblage or concentration. The number of participants has grown steadily over the past three contests, from 15 in 2002 (McCarty, 2002) to 35 in 2004 (Kleeberg, 2005) and 37 in 2006. Details of the previous contests are available at [www.clays.org/reynoldscup.html](http://www.clays.org/reynoldscup.html).

### PREPARATION OF REFERENCE-MINERAL MIXTURES

Three mineral mixtures were prepared from relatively pure reference minerals sourced from commercial and private collections (Table 1). Most of the non-clay minerals came as crystals, which were carefully handpicked. The minerals were crushed using tungsten carbide elements in a percussion mortar and pestle to pass through a 400 µm screen. Coarse impurities in the reference clay mineral standards were removed by dispersing with deionized water or Na hexametaphosphate solution, followed by centrifugation for size

\* E-mail address of corresponding author:  
oomotoso@NRCan.gc.ca  
DOI: 10.1346/CCMN.2006.0540609

Table 1. Reference minerals used to create the three sample mixtures.

Minerals	Empirical formula	Locality
Albite (1)	Ab <sub>98</sub> An <sub>2</sub>	Amelia Courthouse, VA, USA
Albite (2)	Ab <sub>93</sub> An <sub>7</sub>	Villeneuve, Quebec, Canada
Anatase	TiO <sub>2</sub>	Chemical reagent
Aragonite	(Ca <sub>0.99</sub> Sr <sub>0.01</sub> )CO <sub>3</sub>	Clarendon, TX, USA
Calcite	CaCO <sub>3</sub>	Chemical reagent
Chlorite (Mg-clinocllore)	(Mg <sub>9.69</sub> Al <sub>1.87</sub> Mn <sub>0.04</sub> Fe <sup>2+</sup> <sub>0.40</sub> )(Si <sub>5.88</sub> Al <sub>2.12</sub> )O <sub>20</sub> (OH) <sub>16</sub>	Bernstein, Austria
Chlorite (Fe-clinocllore)	(MgAl) <sub>9.56</sub> Fe <sup>2+</sup> <sub>2.44</sub> (Si <sub>5.28</sub> Al <sub>2.72</sub> )O <sub>20</sub> (OH) <sub>16</sub>	Madison County NC, USA
Chlorite (Ripidolite)	(Mg <sub>5.67</sub> Al <sub>2.48</sub> Mn <sub>0.03</sub> Fe <sup>2+</sup> <sub>3.83</sub> )(Si <sub>5.47</sub> Al <sub>2.53</sub> )O <sub>20</sub> (OH) <sub>16</sub>	Flagstaff Hill, El Dorado County, CA, USA
Dolomite	(Ca <sub>0.99</sub> Mg <sub>0.98</sub> Fe <sub>0.02</sub> Mn <sub>0.01</sub> )(CO <sub>3</sub> ) <sub>2</sub>	Haley Station, ON, Canada
Fluorite	CaF <sub>2</sub>	St. Lawrence, NL, Canada
Fluorapatite	Ca <sub>5</sub> (PO <sub>4</sub> ) <sub>3</sub> F	Buckingham, Quebec, Canada
Glauconite-smectite (45:55)	(K <sub>0.72</sub> Na <sub>0.04</sub> )(Al <sub>1.76</sub> Mg <sub>0.46</sub> Fe <sub>1.78</sub> )(Si <sub>7.70</sub> Al <sub>0.30</sub> )O <sub>20</sub> (OH) <sub>4</sub>	Unknown locality in Alberta, Canada
Hematite	Fe <sub>2</sub> O <sub>3</sub>	Guysborough, NS, Canada
Illite RM30*	(K <sub>1.58</sub> Na <sub>0.03</sub> Ca <sub>0.01</sub> )(Al <sub>3.76</sub> Mg <sub>0.24</sub> )(Si <sub>6.60</sub> Al <sub>1.40</sub> )O <sub>20</sub> (OH) <sub>4</sub>	Silverton caldera, CO, USA
Illite-smectite (ISCz-1)	(K <sub>1.01</sub> Na <sub>0.16</sub> Ca <sub>0.03</sub> Mg <sub>0.05</sub> )(Al <sub>3.43</sub> Mg <sub>0.42</sub> Fe <sub>0.15</sub> )(Si <sub>7.11</sub> Al <sub>0.89</sub> )O <sub>20</sub> (OH) <sub>4</sub>	Unknown locality in 'Czechoslovakia'
Kaolinite KGa-1b	(Al <sub>3.95</sub> Ti <sub>0.04</sub> Fe <sub>0.01</sub> )(Si <sub>3.95</sub> Al <sub>0.05</sub> )O <sub>10</sub> (OH) <sub>8</sub>	County of Washington, GA, USA
Kaolinite KGa-2	(Al <sub>3.88</sub> Ti <sub>0.05</sub> Fe <sub>0.07</sub> )(Si <sub>3.97</sub> Al <sub>0.03</sub> )O <sub>10</sub> (OH) <sub>8</sub>	County of Warren, GA, USA
K-spar (adularia)	(K <sub>0.85</sub> Na <sub>0.12</sub> Ba <sub>0.02</sub> Sr <sub>0.01</sub> )Al <sub>1.02</sub> Si <sub>2.98</sub> O <sub>8</sub>	Rhone glacier, Switzerland
Magnesite	(Mg <sub>0.993</sub> Ca <sub>0.004</sub> Fe <sub>0.002</sub> Mn <sub>0.001</sub> )CO <sub>3</sub>	Brumado, Bahia, Brazil
Magnetite	Fe <sub>3</sub> O <sub>4</sub>	Chemical reagent
Montmorillonite (JCSS-3101)	(K <sub>0.02</sub> Na <sub>0.83</sub> )(Al <sub>3.15</sub> Mg <sub>0.65</sub> Fe <sub>0.20</sub> )(Si <sub>7.80</sub> Al <sub>0.20</sub> )O <sub>20</sub> (OH) <sub>4</sub>	Tsukinuno, Japan
Muscovite (1)	(Na <sub>0.15</sub> K <sub>1.75</sub> )(Al <sub>3.69</sub> Mg <sub>0.04</sub> Fe <sub>0.26</sub> )(Si <sub>6.15</sub> Al <sub>1.85</sub> )O <sub>20</sub> (OH) <sub>3.7</sub> F <sub>0.3</sub>	Madras, India
Muscovite (2)	(K <sub>1.73</sub> )(Al <sub>3.70</sub> Mg <sub>0.12</sub> Fe <sub>0.18</sub> )(Si <sub>6.39</sub> Al <sub>1.61</sub> )O <sub>20</sub> (OH) <sub>2.9</sub> F <sub>1.1</sub>	Unknown locality in the USA
Nontronite NAu-1	(Ca <sub>0.3</sub> Mg <sub>0.16</sub> Na <sub>0.06</sub> K <sub>0.01</sub> )(Al <sub>0.38</sub> Mg <sub>0.06</sub> Fe <sub>3.56</sub> )(Si <sub>7.08</sub> Al <sub>0.92</sub> )O <sub>20</sub> (OH) <sub>4</sub>	Uley, South Australia
Oligoclase (1)	Ab <sub>68</sub> An <sub>27</sub> Or <sub>5</sub>	Arendal, Norway
Oligoclase (2)	Ab <sub>78</sub> An <sub>18</sub> Or <sub>4</sub>	Mattawa, ON, Canada
Opal-CT**	Si <sub>0.99</sub> Al <sub>0.01</sub> .0.13H <sub>2</sub> O	Unknown locality in CA, USA
Pyrite	FeS <sub>2</sub>	Huanzala, Peru
Quartz	SiO <sub>2</sub>	Chemical reagent
Rutile	TiO <sub>2</sub>	Graves Mountain, GA, USA
Saponite (JCSS-3501)	Na <sub>0.71</sub> (Mg <sub>5.93</sub> Al <sub>0.07</sub> )(Si <sub>7.22</sub> Al <sub>0.78</sub> )O <sub>20</sub> (OH) <sub>4</sub>	Kunimine, Japan
Serpentine (lizardite-chrysotile)	(Mg <sub>5.99</sub> Fe <sub>0.01</sub> )(Si <sub>3.98</sub> Al <sub>0.02</sub> )O <sub>10</sub> (OH) <sub>8</sub>	Kilmarnock, Quebec, Canada
Siderite	(Fe <sub>0.95</sub> Mn <sub>0.05</sub> )CO <sub>3</sub>	Ivigut, Greenland
Spinel	(Zn <sub>0.9</sub> Fe <sub>0.1</sub> )Al <sub>2</sub> O <sub>4</sub>	Unknown locality, Sri Lanka
Tourmaline (feruvite)	(Ca,Na)(Fe,Mg,Ti) <sub>3</sub> (Al,Mg,Fe) <sub>6</sub> (B <sub>0.5</sub> ) <sub>3</sub> Si <sub>6</sub> O <sub>18</sub> (OH) <sub>4</sub>	Bancroft ON, Canada
Zircon	ZrSiO <sub>4</sub>	Rio do Peixe, Goias, Brazil

\* Eberl *et al.* (1987)

separation. Excess phosphate was removed by repeated ultracentrifugation after rinsing in deionized water. Impurities detectable by conventional XRD were allowed as long as they were unambiguously quantifiable. All the samples were air dried and equilibrated at ~25% RH at between 19 and 21°C. Each mixture (~300 g) was mixed for 24 h in a roller mill and subsequently split into 64 × 4.6 g portions in a laboratory splitter.

Two samples were chosen at random from the 64 and tested for homogeneity using X-ray fluorescence spectroscopy (XRF) and XRD. The XRF data are given in Table 2 and the XRD patterns of the two subsamples of

RC 3-1 are shown in Figure 1. The diffraction patterns were collected on a Bruker D8 Advance with an incident beam parabolic mirror (CoK $\alpha$ ), a 25 mm sample diameter, and a VANTEC-1<sup>TM</sup> linear detector. The XRF data were collected on a Bruker S4 explorer equipped with a wavelength-dispersive spectrometer. Samples were fused in Li metaborate-tetraborate flux and quantified using calibration curves generated from reference standards. Fluorite, fluoroapatite and mica reference minerals were pulverized and analyzed as pressed pellets to enable quantification of fluorine. The elemental composition was used to generate the empirical formulae given in Table 1.

Table 2. Homogeneity test with XRF (wt.% oxide).

	RC 3-1		RC 3-2		RC 3-3	
	A	B	A	B	A	B
Na <sub>2</sub> O	1.90	2.13	0.92	0.90	1.30	1.32
MgO	2.76	2.73	3.39	3.43	10.44	10.44
Al <sub>2</sub> O <sub>3</sub>	20.62	20.42	10.77	10.85	7.30	7.48
SiO <sub>2</sub>	52.31	52.23	50.54	50.49	54.85	54.74
P <sub>2</sub> O <sub>5</sub>	0.00	0.00	1.59	1.59	0.04	0.03
SO <sub>3</sub>	1.08	1.08	0.42	0.42	0.34	0.38
K <sub>2</sub> O	1.80	1.80	0.44	0.44	0.65	0.64
CaO	2.14	2.29	10.33	10.39	0.17	0.15
TiO <sub>2</sub>	3.54	3.48	0.49	0.47	0.40	0.39
MnO	0.04	0.04	0.06	0.06	0.02	0.03
Fe <sub>2</sub> O <sub>3</sub>	3.37	3.36	8.98	9.09	15.37	15.55
ZrO <sub>2</sub>	0.15	0.15	0.00	0.00	0.00	0.00
ZnO	0.00	0.00	0.00	0.00	1.65	1.78
LOI (1000°C)	9.68	9.78	11.57	11.84	6.85	6.88

LOI: loss on ignition

#### SAMPLE COMPOSITION AND SUBMITTED RESULTS

Table 3 gives the compositions of the three sample mixtures created from the reference minerals and the results submitted by the top three entries. Results were ranked based on the sum of the deviations from the actual compositions (total bias) of the three mixtures. The total bias is given in equation 1.

$$\text{Total bias}(\Delta) = \sum \text{abs}(W_{i, \text{actual}} - W_{i, \text{submitted}}) \quad (1)$$

$W_i$  is the weight% of the  $i^{\text{th}}$  mineral. For consistency in mineral nomenclature, certain minerals are grouped together (italics in Table 3). For example, albite and oligoclase are grouped under plagioclase; all 2:1 dioctahedral clay minerals are grouped together but

separated from 2:1 trioctahedral minerals. Misidentified minerals and those making up <0.1 wt.% of the samples were not counted as bias.

Samples RC 3-1 and RC 3-2 comprised five clay minerals and 12 non-clay minerals each. One of the challenges in analyzing these samples was accurate mineral identification given the large number of phases. There were two plagioclases with different chemistries in each sample, which are not easily differentiated by most techniques. Also, differentiating between the 2:1 clay minerals (Al clays in sample 1 and Fe clays in sample 2) was problematic. While almost all participants identified chlorite, large errors were reported possibly because of incorrect approximation of the Fe distribution in the octahedral and hydroxide sheets or incorrect choice of standards. Only one participant correctly

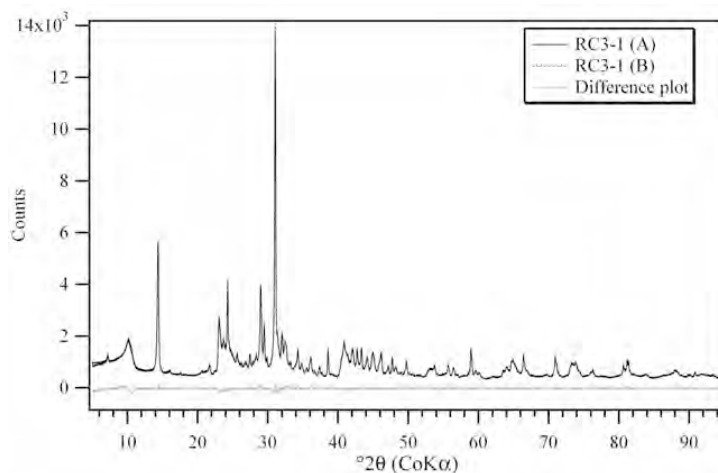


Figure 1. XRD patterns of two randomly chosen RC 3-1 samples for an homogeneity test.

Table 3. Composition (wt.%) of samples RC 3-1 (A), RC 3-2 (B), and RC 3-3 (C). 1<sup>st</sup>, 2<sup>nd</sup> and 3<sup>rd</sup> correspond to the top three entries. For ranking purposes, minerals grouped together are given in italics and the group composition in bold.

A				
Mineral	RC 3-1	1 <sup>st</sup>	2 <sup>nd</sup>	3 <sup>rd</sup>
Quartz	15.5	17.0	16.4	15.7
K-spar (adularia)	4.9	5.0	4.1	5.8
<i>Albite (1)</i>	1.5			
<i>Oligoclase (1)</i>	3.7			5.2
<b>Plagioclase group</b>	<b>5.2</b>	<b>6.0</b>	<b>5.4</b>	<b>5.2</b>
Calcite	2.1	2.0	1.9	2.8
Dolomite	2.0	2.0	1.7	2.2
Siderite	1.0	1.0	0.6	1.4
Tourmaline	1.5			2.0
Pyrite	2.8	3.0	2.4	2.5
Anatase	1.8	2.0	1.9	2.3
Rutile	1.8	2.0	1.4	1.9
Zircon	0.2			0.4
Kaolinite (KGa-1b)	25.3	27.0	28.3	26.2
<i>Illite (RM-30)</i>	8.2	10.0		6.2
<i>Illite-smectite (ISCz-1)</i>	4.8		20.0	
<i>Na-montmorillonite</i>	18.8	20.0	13.0	22.5
<b>Total dioctahedral 2:1 clay</b>	<b>31.7</b>	<b>30.0</b>	<b>33.0</b>	<b>28.7</b>
Mg-clinochlore	4.1	3.0	2.7	2.9
B				
Mineral	RC 3-2	1 <sup>st</sup>	2 <sup>nd</sup>	3 <sup>rd</sup>
Quartz	29.9	31.0	29.4	31.6
<i>Albite (2)</i>	6.1			
<i>Oligoclase (2)</i>	2.5			
<b>Plagioclase group</b>	<b>8.6</b>	<b>9.0</b>	<b>7.8</b>	<b>7.2</b>
Calcite	4.6	4.0	4.7	4.7
Aragonite	4.0	4.0	4.3	5.3
Dolomite	3.0	3.0	2.9	3.2
Magnesite	3.0	3.0	2.8	3.7
Siderite	1.4	1.5	1.7	1.2
Fluorite	2.8	3.0	2.3	2.8
Apatite	4.0	4.0	2.8	3.3
Hematite	3.1	4.0	3.4	3.0
Goethite	0.1			
Ilmenite	0.1			
Anatase	0.2			
Kaolinite (KGa-2)	15.0	16.0	13.7	17.4
<i>Muscovite 2M<sub>1</sub> (1)</i>	2.4	4.5	1.9	4.5
<i>Glauconite-smectite (45:55)</i>	3.6			
<i>Nontronite</i>	7.2	5.0	14.6	8.8
<b>Total dioctahedral 2:1 clay</b>	<b>13.2</b>	<b>9.5</b>	<b>16.5</b>	<b>13.3</b>
Fe-rich chlorite (ripidolite)	7.0	8.0	6.9	3.3

identified zircon and tourmaline (minor phases) in sample RC 3-1. Mixed-layer illite-smectite in sample RC 3-1 and glauconite-smectite in sample RC 3-2 were seldom reported. Sample RC 3-3 was perhaps the most difficult despite containing only 10 phases. The presence of poorly crystalline opal-CT in a mixture with opal-A

and a 2:1 trioctahedral clay mineral (saponite) made quantification of either phase difficult.

Almost all the participants quantified the minerals from laboratory XRD data using standard analysis techniques (Table 4). The more successful (and some unsuccessful) entries, however, made use of a wide range

Table 3 (contd.)

Mineral	RC 3-3	1st	2nd	3rd
Quartz	2.1	3.0	2.3	4.0
Opal-CT*	35.7	37.0	30.7	29.5
Magnetite	6.4	7.0	7.1	7.2
Hematite	7.4	5.0	7.3	7.6
Ilmenite	0.6	1.0	0.5	0.6
Spinel	5.1	6.0	3.7	4.2
Lizardite/chrysotile	3.2	2.0	2.1	1.7
Muscovite 2M <sub>1</sub> (2)	6.1	7.0	4.0	4.4
Saponite	28.9	25.0	38.5	38.0
Fe-clinochlore	4.5	7.0	3.4	2.8

\* contains minor amounts of opal-A.

of supplementary techniques including elemental analysis, grain-size or magnetic separation, infrared spectroscopy, and thermogravimetric analysis. One participant used Mössbauer spectroscopy to correctly identify most of the Fe-bearing minerals. It was striking to note that most of the participants employed the Rietveld method for quantification with varying degrees of success. This suggests a tendency by less experienced analysts to use Rietveld refinement programs as a 'black box' for quantification. It is also interesting to see that only one participant tried to quantify clay minerals (albeit unsuccessfully) from a single-line XRD method using oriented sample preparations. In spite of the limitations of the method in complex mineral assemblages, it is still popular in soil science and sedimentology.

Details of the quantitative methods employed by the top three contestants are discussed below.

#### Single-line matrix flushing – method applied by contest winner (P31)

Clay minerals were identified from diagnostic *hkl d* values and the XRD patterns of treated oriented aggregates derived from the centrifuged supernatant solution. Non-clay minerals were identified from diffraction data of a randomly oriented aggregate of the bulk sample using the ICDD PDF-4 database and Jade<sup>TM</sup> (MDI) or other literature and computing sources. Cation exchange capacity and thermogravimetric analysis were also used as supplementary identification techniques.

Approximately 2.7 g of sample were combined with 0.3 g of reagent-grade ZnO to give a 10% spike. The mixture was ground in a McCrone micronizing mill for 5 min in 4–6 mL of hexane. After evaporation of hexane, the mixture was passed through a 400 µm sieve and side-loaded into a 25 mm sample holder. Diffraction data (CuKα radiation) were collected on a θ-θ Bruker D8 Advance<sup>TM</sup> diffractometer equipped with a Solex<sup>TM</sup> solid-state Peltier detector, counting from 5 to 65°2θ with a 0.02°2θ step at 60 s per step. The Bragg-Brentano optics includes 2 mm (1°) fixed divergent and antiscatter slits, and 0.6 mm receiving slit.

A modification of the single-line matrix-flushing technique (Chung, 1974a) was used for quantification. The basic equations for calculating the amount of a mineral (%X) are given in equations 2 and 3.

$$\%X = \frac{I_x \mu_m^*}{K_x} \quad (2)$$

$I_x$  is the intensity of the mineral  $x$  chosen reflection,  $\mu_m^*$  is the mass attenuation coefficient of the mixture, and  $K_x$  is a phase-dependent constant. By using an internal standard (S), a reference intensity ratio (RIR) is defined such that  $K_x$  and  $\mu_m^*$  are eliminated:

$$\%X = \frac{I_x \times M_s \times 100}{I_s \times M \times RIR} \quad (3)$$

$I_s$  is the intensity of the chosen reflection of the internal standard,  $M_s$  is the mass of the internal standard and  $M$  is the mass of the unknown sample.

Instead of decomposing peaks in the observed pattern to obtain integrated intensities, diffraction patterns of reference standards were collected using the same conditions as those used for the unknown sample. The standard patterns were fitted to the observed pattern using a genetic algorithm program (in-house Chevron program QUANTA<sup>TM</sup>). The technique employs a weighted whole-pattern fitting procedure, strengthening the weights assigned to diagnostic regions and assigning low weights to (or excluding) diffracted intensities more sensitive to structural and chemical variations (Mystkowski *et al.*, 2002) such as the low-angle scan region with strong basal reflections from layer silicates. Usually, the region above 4.6 Å is excluded from fitting to avoid the effects of preferred orientation on the clay basal peaks. The strongest quartz and zincite peaks are excluded to avoid beam saturation problems from non-linear detector response. The technique also uses the strong peaks of clay mineral groups between 1.48 and 1.55 Å for the diagnostic single-line reflection. These peaks are most often the 060 reflections. The most variable parameter is Fe content, which defines the  $d$  value of groups within 2:1 layer dioctahedral clays and mica. The QUANTA<sup>TM</sup> full-pattern fits are shown in Figures 2–4. The full-pattern fitting procedure is used only to obtain the most accurate measure of the integrated intensity of the diagnostic reflection chosen for the single-line concentration calculation. Care was taken to choose the single lines for each mineral to minimize resulting RIR variation that may result from structural imperfections and ionic substitution.

Care was also taken to physically keep mass absorption comparable when measuring the mineral intensity factors for the diagnostic reflections of reference minerals by preparing non-clay minerals with kaolinite and the zincite internal standard. Clay mineral standards were prepared with quartz and the zincite internal standard. As long as the reference mineral standard is comparable to that in the unknown, the

Table 4. Analytical methods used by participants.

Participant no.	Total bias	XRD single line	XRD pattern summation	XRD Rietveld	XRD, oriented samples	Grain-size separation	Magnetic separation	Chemical analysis	SEM (or TEM)-EDX	IR spectroscopy	TG-DTA-DSC	CEC	Petrography	Mössbauer
31	33.8	x	x	+	+	+		x			+	+		
18	41.7		x		+	+								
4	45.9			x	+				+					
15	50.2			x	+	+	+	x	+	+		+		
9	51.6			x	+	+	+							
40	53.4			x				x						
10	54.9		x											
32	59.0		x		+								+	
5	60.1			x	+	+				+				
14	66.7			x	+	+		+		+	+	+		
23	99.7			x										
30	103.6	x			+	+								
24	113.5			x										
19	116.7			x										
56	121.1			x						+	x			
47	122.3	x			+						+		+	
22	123.3	x			+									
50	126.2													
3	126.7			x	+	+	+		+					
43A	130.8			x	+									
36	137.0	+							x					
43	139.0			x	+									
41	152.0	x			+	x								
38	168.4	x	x											x
1	169.1	x												
34	173.9			x					x					
27	179.3			x				x						
57	190.7			x										
21	192.3	x			x	x					x			
54	194.6			x	+				x					
37	197.6	x						x						
25	206.7	x			+	+			x					
49	212.2	x			+									
28	219.7	x			+			+	x	+				
35	253.2			x				x						
52	278.0			x										
26	300.0			x					x					

x methods used for quantification

+ supplementary methods

program can effectively fit what is often a series of overlapping reflections. In samples RC 3-1 and RC 3-2, illite-smectite and glauconite-smectite were misidentified, causing an underestimation of the total 2:1 layer dioctahedral clays. Also in sample RC 3-3, both the hematite and magnetite standards are different from those in the sample, resulting in a larger-than-normal error in composition. Elemental composition optimization was used separately to constrain phase concentrations that were uncertain because the reference mineral

standards were lacking or not ideal. Elemental composition obtained from XRF is comparable to the actual composition given in Table 2. This part of the analysis was made using an in-house Chevron program, BESTMIN<sup>TM</sup>, which optimizes oxide data with quantitative phase analysis (QPA) data using QUANTA<sup>TM</sup> (Środoń *et al.*, 2006). For example, Fe oxide phases in RC 3-3 were highly uncertain from the QUANTA<sup>TM</sup> analysis alone. BESTMIN<sup>TM</sup> allowed limits to be set for the total Fe oxide mineral concentration based on

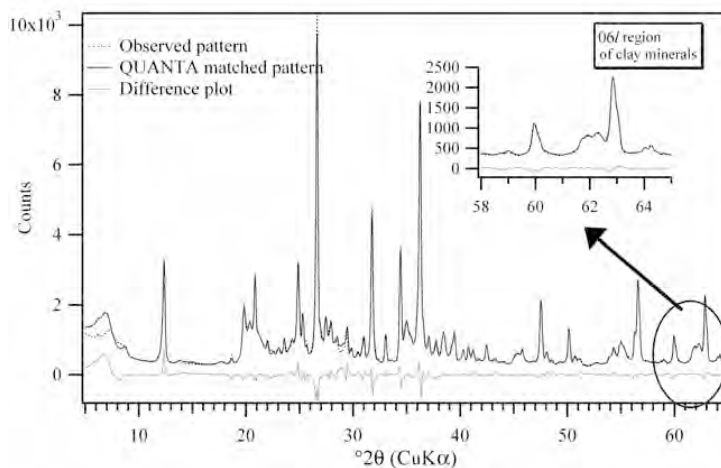


Figure 2. QUANTA whole-pattern fit to sample RC 3-1.

available  $\text{Fe}_2\text{O}_3$  from the XRF data. The high concentration of  $\text{MgO}$  determined from XRF in conjunction with the  $d_{060}$  was used to positively identify saponite and optimize the concentration obtained using QUANTA<sup>TM</sup>.

In addition to these fundamental strategies, numerous replicate XRD scans and quantifications were made from fresh sample preparations in order to evaluate and minimize preferred orientation and ensure good counting statistics.

*Whole-pattern fitting – the method applied by second-place finisher (P18)*

The as-received samples were carefully split into two portions weighing ~2 g each. One portion of each sample was placed in a McCrone mill together with an appropriate amount of ethanol and the mixture was

milled for 12 min. Ethanol was chosen as the slurry liquid rather than water to allow spray-drying at a lower temperature in case the samples contained temperature-sensitive phases such as sulfates. The resulting slurries were spray dried directly from the mill at a temperature of 60°C (Hillier, 1999, 2002). The spray-dried powder samples were top-loaded into 25 mm circular cavity holders and diffraction patterns were collected on a Siemens D5000 diffractometer using  $\text{CoK}\alpha$  radiation selected by a diffracted beam monochromator. The beam was collimated with 1° divergence and antiscatter slits and a 0.6 mm receiving slit. Samples were scanned from 2 to 75°2θ in 0.02° steps, counting 30 s per step. Additionally, in order to aid identification of the clay minerals present in the samples, 200 mg of the remaining sample portion were dispersed ultrasonically and

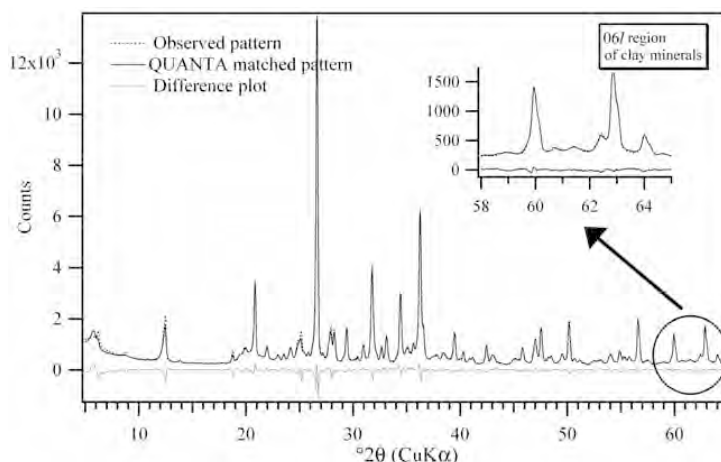


Figure 3. QUANTA whole-pattern fit to sample RC 3-2.

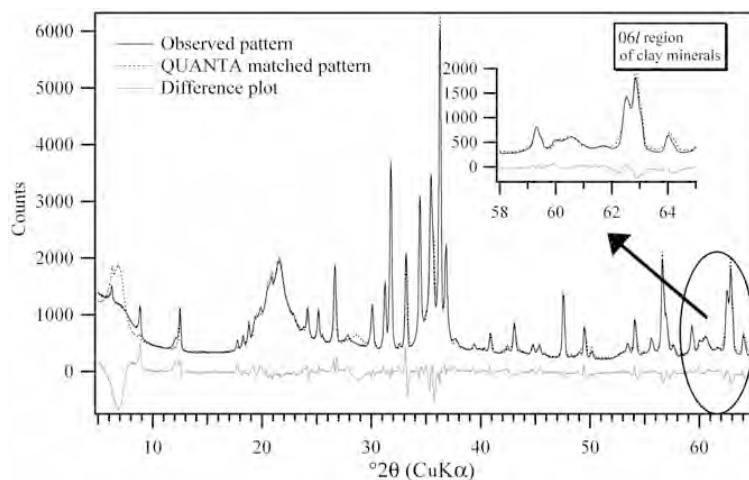


Figure 4. QUANTA whole-pattern fit to sample RC 3-3.

<2 μm fractions were obtained by timed sedimentation. These subsamples were prepared as oriented mounts using the filter peel method and scanned in the air-dried state, after ethylene glycol solvation by vapor pressure overnight followed by heating at 300°C for 1 h. These scans were recorded from 2 to 45°2θ in 0.02° steps, counting 1 s per step.

Qualitative analysis was the first step used to identify the phases present in the samples and was accomplished using reference patterns from the ICDD powder diffraction file and Bruker Diffrac Plus EVA<sup>TM</sup> software, together with consideration of data from the <2 μm clay fraction analysis. Quantitative analysis was made only on the bulk spray-dried samples using full-pattern fitting. Standard reference patterns were prepared by spray-drying mineral phases as pure samples and as samples spiked with 50 wt.% corundum as an intensity reference. Where necessary, detectable impurities were subtracted electronically from the reference patterns and allowance was made for their concentration in the spiked standards when calculating full-pattern RIRs. The full-pattern fitting was done using an EXCEL<sup>TM</sup> spreadsheet and the SOLVER<sup>TM</sup> add-in to minimize an objective function dependent on the difference between the observed diffraction pattern and a pattern composed of a sum of single-phase reference patterns. For these samples, the objective function ( $R$ ), which is also the reliability of the fit, was the least-squares error criterion, as given in equation 4 (Howard and Preston, 1989):

$$R = \left\{ \frac{\sum [I_{2\theta_i}^{\text{obs}} - I_{2\theta_i}^{\text{calc}}]^2}{\sum [I_{2\theta_i}^{\text{obs}}]^2} \right\}^{1/2} \quad (4)$$

where  $2\theta_i$  is the  $i^{\text{th}}$  data point observed (obs) or calculated (calc). The spreadsheet-based method is essentially a

variant of those implemented in FULLPAT (Chipera and Bish, 2002) and ROCKJOCK (Eberl, 2003) spreadsheets. In the first cycle of the fitting process, the proportions of the reference patterns were allowed to vary; in the second cycle, all patterns, including the unknown, were allowed to shift independently by a fraction of a step ( $\pm 0.02^\circ$ ) along  $2\theta$ ; in the third and final cycle the proportions were again allowed to vary. Shifts along  $2\theta$  were accommodated by a cubic spline function, as suggested for differential XRD by Schulze (1986). Several fitting runs were made for each sample. By this means, trace phases which had not been recognized initially were added and/or different reference patterns of the same phase were tried in attempts to improve the fit. For some phases, several reference patterns of the same phase were used simultaneously to aid in accounting for differences between the phases present in the samples and the standards. The region below 11.3 Å was excluded from the calculations because of the variability in the position and intensity of clay mineral peaks in this region due to factors such as the state of hydration. The final values of the objective function for samples RC 3-1, RC 3-2, and RC 3-3 were 6.15, 3.58, and 6.15, respectively. Since no internal standard was added to the unknown sample, phase abundance ( $X_i$ ) was calculated from the proportion of each reference pattern required to make the fit and the whole-pattern RIR. This was accomplished using a normalized RIR method (Hillier, 2003) given by equation 5 whereby full-pattern proportion replaces a single peak as the measure of intensity. Small amounts of corundum (0.5–1%) originating from the abrasion of mill rods were normalized out of the results.

$$X_i = \left( \frac{\text{RIR}}{I_{(\text{pattern})i}} \sum_{i=1}^n \frac{I_{(\text{pattern})i}}{\text{RIR}} \right)^{-1} \quad (5)$$



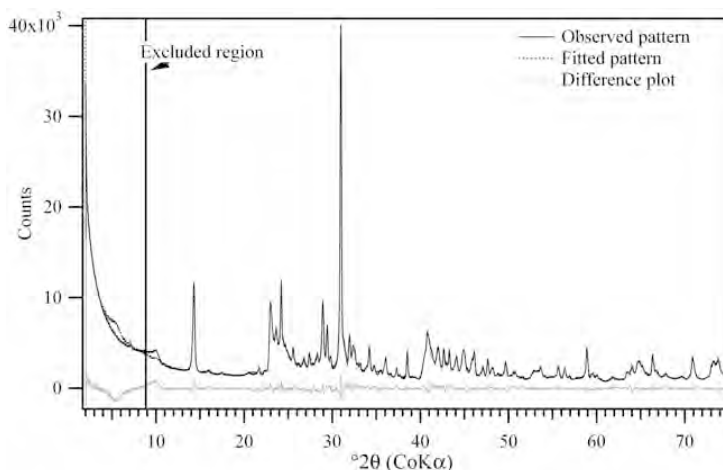


Figure 5. Whole-pattern fits of spray-dried RC 3-1.

Where  $I_{(pattern)i}$  denotes the intensity (proportion) of a specific pattern of mineral  $i$  required by the fit. This method is also sometimes known as the 'adiabatic' method after Chung (1974b) (adiabatic – nothing lost, nothing gained) but 'normalized RIR method' is the preferred name (Jenkins and Snyder, 1996). The whole-pattern fits are shown in Figures 5–7.

*Rietveld analysis – method applied by third-place finisher (P4)*

The application of Rietveld analysis to quantification of clay minerals has been limited primarily due to the difficulty in describing refineable structures for disordered phyllosilicates (Bish and Post, 1993). For these samples, models were used to describe disorder as described by Bergmann and Kleeberg (1998) and Ufer *et al.* (2004).

Precisely 2.7 g of sample and 0.3 g of zincite (internal standard) were ground with 10 mL of ethanol for 8 min in a McCrone micronizing mill using agate-grinding elements. The slurry was air dried and homogenized with small steel balls in a vibrating mill. The powder was side-loaded into the holders and measured with a Seifert URD-6 diffractometer using  $\text{CoK}\alpha$  at 40 kV and 30 mA. The diffractometer is equipped with a theta compensating divergence slit (15 mm sample length irradiated) and graphite monochromator. Diffraction data were collected from 5 to  $80^\circ 2\theta$  in  $0.02^\circ$  steps, counting 15 s per step.

For clay mineral identification, oriented samples were prepared by drying a suspension on glass slides, without previous size fractionation. Diffraction data were collected for air-dried sample, glycolated sample, sample heated to  $400^\circ\text{C}$ , and sample heated to  $550^\circ\text{C}$ , using the same slide.

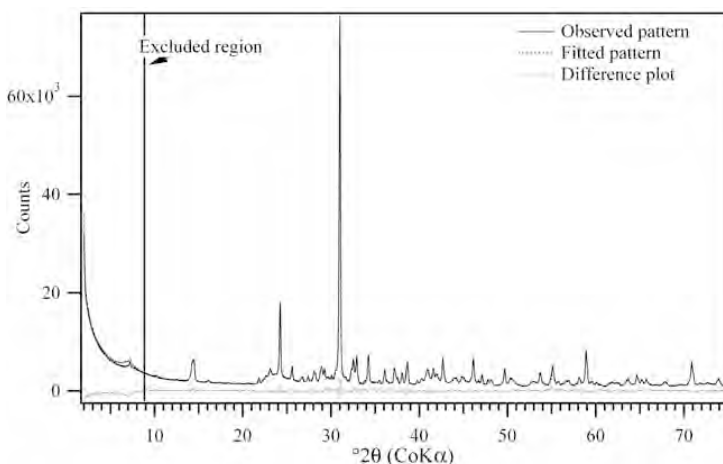


Figure 6. Whole-pattern fits of spray-dried RC 3-2.

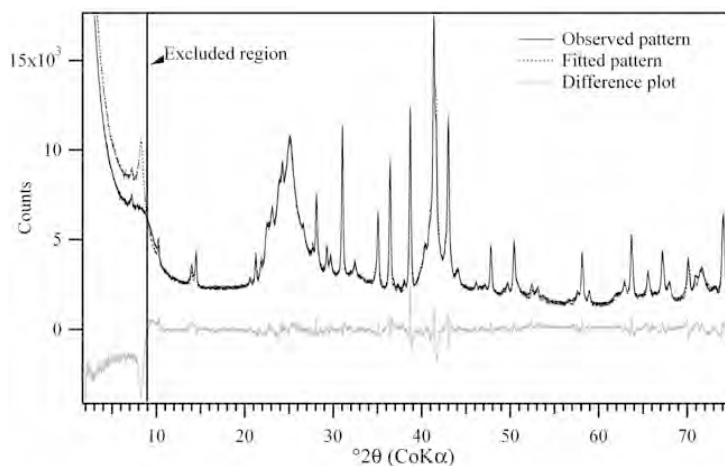


Figure 7. Whole-pattern fits of spray-dried RC 3-3.

Mineral identification in the random preparations was conducted using ANALYZE<sup>TM</sup> and PDF-2. The Rietveld program AUTOQUAN (GE Inspection Technologies), was used for quantification and minor phases were identified by PC-PDF from the remaining maxima in the Rietveld difference plot.

The following generalized refinement model was adopted for all three samples:

Background was modelled by a 3- or 4-parameter polynomial; zero point (limits  $\pm 0.01^\circ$ ) and sample displacement (limits  $\pm 0.2$  mm) were always refined

Lattice parameters were refined for all phases with 'reasonable' interval restraints. However, the  $\beta$  parameter of the monoclinic structure of the 2:1 layers of smectites was fixed because of disordering; all atomic coordinates and displacement parameters were kept fixed; a number of occupancy parameters was refined, within predefined limits, e.g., interlayer K in mica was limited to 0.8–1 and 0.6–0.9 in illites, interlayer complex (cation and water) in smectites was limited to 0.2–0.4, Mg and Fe in chlorites were distributed on three octahedral positions, and Fe was substituted for Al in the octahedral sheet of dioctahedral smectites. Also Fe occupancy was refined in the tetrahedral sheet of nontronite as well as *cis-trans* distribution in dioctahedral smectites.

Isotropic size-related line broadening was assumed for all non-clay minerals and mica. For minerals with solid-solutions like plagioclase, a microstrain-related parameter was added.

Kaolinite and chlorite were described by a 2-subphase disordering model (Bergmann and Kleeberg, 1998). For smectites, the 'single-layer approach' (Ufer *et al.*, 2004) was used for fitting the turbostratic structures.

Spherical harmonics models were used to correct preferred orientation, which was observed especially for coarse-grained layer silicates, but also for feldspar and carbonate phases.

Altogether, 175 (sample RC 3-3) to 225 parameters (sample RC 3-2) had to be refined. This was performed in full-automatic mode without analyst intervention. The main criterion for accepting the QPA result was the closeness of the X-ray amorphous mineral content to zero (difference from 100%, all phases related to spiked internal standard).

*Sample-specific problems.* In sample RC 3-1, the presence of the minor phases tourmaline and zircon was confirmed by SEM-EDX. The difference plot of the Rietveld fit, in Figure 8, did show a 10.6 Å hump due to illite-smectite but was misinterpreted as dehydrated smectite because of poor control of humidity in the laboratory. Consequently, the smectite and illite models did not compensate for all the remaining intensity of illite-smectite, so the sum of 2:1 clay minerals is underestimated by 3%. The very flexible kaolinite model did compensate for some of the intensity, so kaolinite was overestimated slightly.

The results could be improved by restricting some broadening parameters and using a simpler broadening model for chlorite. Size fractionation might have helped to distinguish the mixed-layered 2:1 clay minerals. The gratifying low bias notwithstanding, the analysis could be improved given a model for the structure of the mixed-layer mineral.

As in sample RC 3-1, the mixed-layered glauconite-smectite in RC 3-2 (Figure 9) was misidentified. Incidentally, the deviations of nontronite and muscovite did compensate for that error. The disordered model for kaolinite did again compensate for intensity from the mixed-layer mineral, and an overestimation of the kaolinite resulted. The result could be improved by narrowing the restraint for line broadening of aragonite, introducing a second plagioclase, and using a simplified model for chlorite. As stated for sample RC 3-1, a model for the mixed-layer minerals is needed.

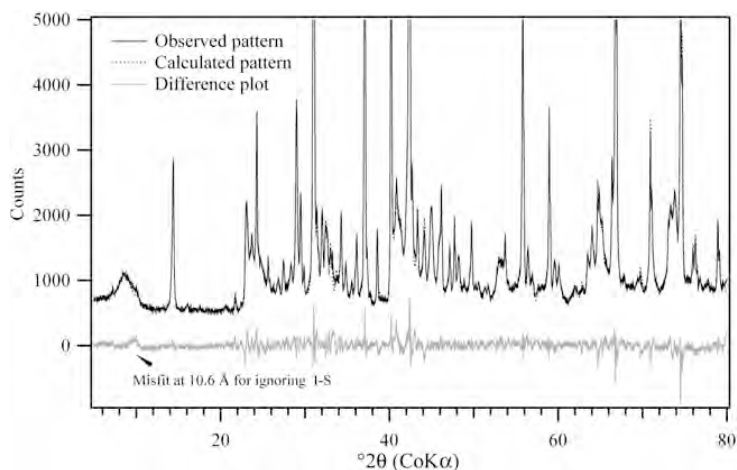


Figure 8. Diffraction plots after Rietveld analysis of sample RC 3-1.

In sample RC 3-3 (Figure 10), a preliminary saponite model was built by modifying the cell parameters and occupancies of a dioctahedral smectite. Opal-CT was modeled using the silica glass structure of Le Bail (1995), plus a tridymite structure. This model was clearly inadequate and yielded incorrect values for saponite and opal by correlation. Better results would have been obtained by building a saponite model from the phlogopite structure, including constrained  $a$  and  $b$  lattice parameters. As a compromise for modeling opal-CT, a mixture of cristobalite and tridymite with prominent line broadening could be used and the opal content defined as the sum of both silica phases plus the 'amorphous' content. However, a stable structural model for opal-CT is needed for better quantification.

#### SUMMARY

Overall, the top 10 participants did an excellent job of quantifying the phases. It is apparent that established XRD methods can be applied successfully to mineral analysis as long as the minerals are accurately identified. Care must be taken when selecting the beam path optics to ensure good counting statistics and resolution to help mineral identification and quantification. The major differences between the top finishers' diffraction patterns for the same samples reflect variations in the use of internal standards and sample preparation (giving rise to differences in preferred-orientation magnitude) and the use of fixed or theta-compensating divergence slits. Ambient humidity may have affected the nature of the interlayer water of smectites and mixed-layer clays (at

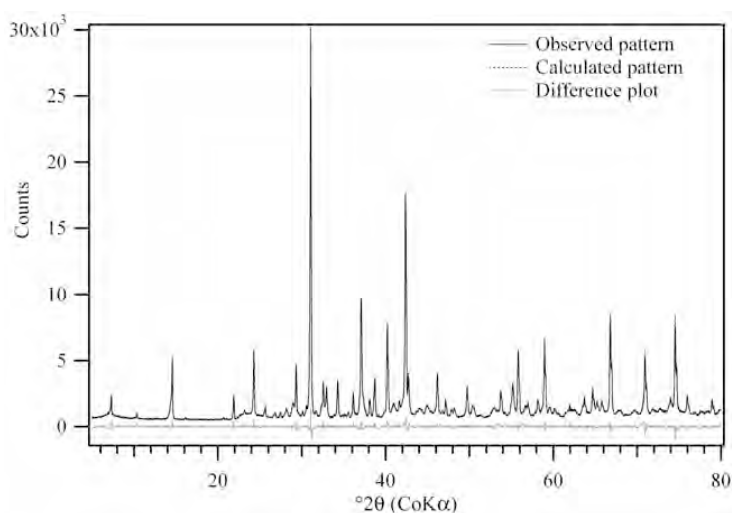


Figure 9. Diffraction plots after Rietveld analysis of sample RC 3-2.

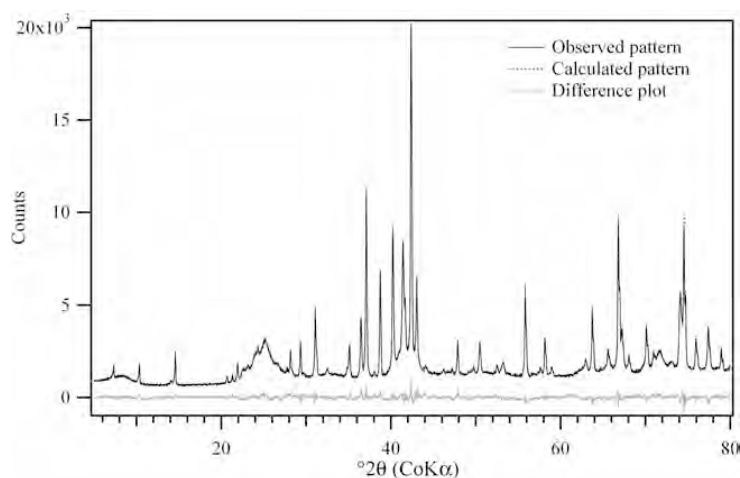


Figure 10. Diffraction plots after Rietveld analysis of sample RC 3-3.

low angles). Such differences highlight the fact that to get the best quantitative results from XRD data of clay-bearing minerals, one must be able to account for both instrumental and environmental factors within the laboratory.

Reducing the particle size by micronizing with a liquid maintains the structural integrity of the phases while significantly reducing absorption contrast effects. It was demonstrated that the single-line RIR method, which is often plagued by preferred orientation and peak overlap issues, can be applied successfully if care is taken in sample preparation and integrated intensities are measured directly from fitted mineral standards instead of the observed pattern. The peaks used should be those for which the intensities are least susceptible to compositional variations or structural disorders such as the  $d_{061}$  of clay minerals. The use of spray-dried samples eliminates preferred orientation and significantly improves the RIR and Rietveld methods for quantification. In general, both single-line and whole-pattern fitting RIR techniques could be applied to crystalline and X-ray amorphous components. Accuracy obtained with the RIR methods would be greatly improved if the standards used were close to the true composition. The effort expended in obtaining and measuring appropriate standards is a key factor for the successful application of standard-based approaches. The reference standards used by the top two finishers were collected over several years from commercial and private sources.

The Rietveld method continues to evolve for mineral quantification of clay-bearing rocks. Structural databases are available from commercial and free sources and structural parameters could easily be refined or constrained to known values to reflect compositional variations typically found in minerals. Such information can be stored in databases or collections of starting structure models, which are easily transferable to other

users or instruments. The main limitation is the expertise required to choose appropriate models and to identify over-parameterized ones. Careful inspection of the results for physically meaningless values of the line broadening and preferred orientation corrections, phase-specific  $R$  values as well as a check of the correlation matrix are key to improving the quality of Rietveld quantification.

Supplementary techniques, especially elemental analysis, are essential for mineral identification and choosing the right standard to use for quantification. It was also demonstrated that the mineral composition can be optimized by knowledge of the elemental composition.

#### ACKNOWLEDGMENTS

The contest organizer would like to thank Wally Friesen and Kirk Michaelian, both of Natural Resources Canada in Devon, for conducting the thermogravimetric and spectroscopic analyses of the reference minerals. The authors would like to thank Natural Resources Canada and The Clay Mineral Society for funding the contest. Stephen Hillier acknowledges the support of the Scottish Executive Environmental and Rural Affairs Department. Douglas McCarty thanks Chevron ETC for financial support, and his colleagues who participated in the 2006 Reynolds Cup contest: Victor Drits, Boris Sakharov, Kym Correll, Russell Anderson and Bruce McCollom. Steve Chipera (Los Alamos, USA) and Reiner Dohrmann (BGR, Germany) are thanked for their constructive reviews. We thank all the contestants who were brave enough to meet the challenge and test their methods.

#### REFERENCES

- Bergmann, J. and Kleeberg, R. (1998) Rietveld analysis of disordered layer silicates. *Materials Science Forum*, **278–281**(1), 300–305.
- Bish, D.L. and Post, J.E. (1993) Quantitative mineralogical analysis using the Rietveld full-pattern fitting method. *American Mineralogist*, **78**, 932–940.
- Chipera, S.J. and Bish, D.L. (2002) FULLPAT: A full-pattern

- quantitative analysis program for X-ray powder diffraction using measured and calculated patterns. *Journal of Applied Crystallography*, **35**, 744–749.
- Chung, F.H. (1974a) Quantitative interpretation of X-ray diffraction patterns of mixtures. I. Matrix-flushing method for quantitative multicomponent analysis. *Journal of Applied Crystallography*, **7**, 519–525.
- Chung, F.H. (1974b) Quantitative interpretation of X-ray diffraction patterns of mixtures. II. Adiabatic principles of X-ray diffraction analysis of mixtures. *Journal of Applied Crystallography*, **7**, 526–531.
- Eberl, D.D. (2003) User's guide to Rockjock – a program for determining quantitative mineralogy from powder X-ray diffraction data. *US Geological Survey Open-File Report* 03-78.
- Eberl, D.D., Środoń, J., Lee, M., Nadeau, P.H. and Northrop, H.R. (1987) Sericite from Silverton caldera, Colorado: correlation among structure, composition, origin, and particle thickness. *American Mineralogist*, **72**, 914–934.
- Hillier, S. (1999) Use of an air-brush to spray dry samples for X-ray powder diffraction. *Clay Minerals*, **34**, 127–135.
- Hillier, S. (2002) Spray drying for X-ray powder diffraction specimen preparation. *IUCr CPD Newsletter*, **27**, 7–9.
- Hillier, S. (2003) Quantitative analysis of clay and other minerals in sandstones by X-ray powder diffraction (XRPD). Pp. 213–251 in: *Clay Minerals Cements in Sandstones* (R.H. Worden and S. Morad, editors). Special Publication **34**, International Association of Sedimentologists.
- Howard, S.A. and Preston, K.D. (1989) Profile fitting of powder diffraction patterns. Pp. 217–275 in: *Modern Powder Diffraction* (D.L. Bish and J.E. Post, editors). Reviews in Mineralogy, **20**, Mineralogical Society of America, Washington, D.C.
- Jenkins, R. and Snyder, R.L. (1996) *Introduction to X-ray Powder Diffractometry*. John Wiley and Sons, New York.
- Kleeberg, R. (2005) Results of the second Reynolds Cup contest in quantitative mineral analysis. *IUCr CPD Newsletter*, **30**, 22–26.
- Le Bail, A. (1995) Modelling the silica glass structure by the Rietveld method. *Journal of Non-Crystalline Solids*, **183**, 39–42.
- McCarty, D.K. (2002) Quantitative mineral analysis of clay bearing mixtures: The Reynolds Cup contest. *IUCr CPD Newsletter*, **27**, 12–16.
- Mystkowski, K., Środoń, J. and McCarty, D.K. (2002) Application of evolutionary programming to automatic XRD quantitative analysis of clay-bearing rocks. *The Clay Minerals Society 39th Annual Meeting, Boulder, Colorado, Abstracts with Programs*.
- Schulze, D.G. (1986) Correction of mismatches in 2θ scales during differential X-ray diffraction. *Clays and Clay Minerals*, **34**, 681–685.
- Środoń, J., Mystkowski, K., McCarty, D.K. and Drits, V.A. (2006) BESTMIN: A computer program for refining the quantities and the chemical composition of clays and other mineral components of fine-grained rocks. *International Conference 'Clays and Clay Minerals' Pushchino, Russia 26–30 June, 2006, Abstracts with Programs*.
- Ufer, K., Roth, G., Kleeberg, R., Stanjek, H., Dohrmann, R. and Bergmann, J. (2004) Description of X-ray powder pattern of turbostratically disordered layer structures with a Rietveld compatible approach. *Zeitschrift für Kristallographie*, **219**, 519–527.

(Received 3 August 2006; revised 31 August 2006; Ms. 1202)